

## Review

## Dune recovery after storm erosion on a high-energy beach: Vougot Beach, Brittany (France)

Serge Suanez <sup>a,\*</sup>, Jean-Marie Cariolet <sup>a</sup>, Romain Cancouët <sup>b</sup>, Fabrice Ardhuin <sup>c</sup>, Christophe Delacourt <sup>b</sup><sup>a</sup> GEOMER - UMR 6554 CNRS LETG, Institut Universitaire Européen de la Mer, Place Nicolas Copernic, 29280 Plouzané, France<sup>b</sup> Domaines Océaniques, DO - UMR 6538 CNRS, Institut Universitaire Européen de la Mer, Place Nicolas Copernic, 29280 Plouzané, France<sup>c</sup> IFREMER, Laboratoire d'Océanographie Spatiale, BP70, 29280 Plouzané, France

## ARTICLE INFO

## Article history:

Received 21 March 2011

Received in revised form 8 October 2011

Accepted 10 October 2011

Available online 23 October 2011

## Keywords:

Coastal dune

Dune recovery

Dune toe accretion

Dune crest retreat

Storm surge

Extreme water levels

Accommodation space

## ABSTRACT

On 10th March 2008, the high energy storm Johanna hit the French Atlantic coast, generating severe dune erosion on Vougot Beach (Brittany, France). In this paper, the recovery of the dune of Vougot Beach is analysed through a survey of morphological changes and hydrodynamic conditions. Data collection focused on the period immediately following storm Johanna until July 2010, i.e. over two and a half years. Results showed that the dune retreated by a maximum of almost 6 m where storm surge and wave attack were the most energetic. Dune retreat led to the creation of accommodation space for the storage of sediment by widening and elevating space between the pre- and post-storm dune toe, and reducing impacts of the storm surge. Dune recovery started in the month following the storm event and is still ongoing. It is characterised by the construction of “secondary” embryo dunes, which recovered at an average rate of 4–4.5 cm per month, although average monthly volume changes varied from  $-1$  to  $2\text{ m}^3\cdot\text{m}^{-1}$ . These embryo dunes accreted due to a large aeolian sand supply from the upper tidal beach to the existing foredune. These dune-construction processes were facilitated by growth of vegetation on low-profile embryo dunes promoting backshore accretion. After more than two years of survey, the sediment budget of the beach/dune system showed that more than  $10,000\text{ m}^3$  has been lost by the upper tidal beach. We suggest that seaward return currents generated during the storm of 10th March 2008 are responsible for offshore sediment transport. Reconstitution of the equilibrium beach profile following the storm event may therefore have generated cross-shore sediment redistribution inducing net erosion in the tidal zone.

© 2011 Elsevier B.V. All rights reserved.

## 1. Introduction

Since the 1960s, several studies based on theoretical or experimental approaches have analysed processes of dune erosion in storm conditions (Edelman, 1968, 1972; van der Meulen and Gourlay, 1968). They have shown the respective roles of the different factors involved in dune erosion such as morphology, sedimentology or hydrodynamics (van de Graaff, 1977; Vellinga, 1982; Kriebel and Dean, 1985; Kriebel, 1986; Carter and Stone, 1989; Carter et al., 1990; Pye and Neal, 1994; Saye et al., 2005; Claudino-Sales et al., 2008). The first work based on a probabilistic approach demonstrated that the “submersion” parameter, determined by the extreme water level at the coast due to a combination of the high spring tide and the storm surge, was the primary factor involved in the dune erosion process (van de Graaff, 1986). More recently, studies applying a

model-based approach to dynamic processes have been carried out, taking into account the impact of run-up on the dune front (Fisher and Overton, 1984; Larson et al., 2004; Erikson et al., 2007). The total dune retreat, and hence volume of sand eroded, therefore depends on the frequency and intensity of each run-up event when its height is greater than that of the dune toe (Overton and Fisher, 1988). This process therefore causes dune undercutting which, in the long run, will lead to destabilisation of the scarp slope. This impact can easily be identified by the presence of erosion features such as beam-type by tensile failures, slumps or slides (Carter and Stone, 1989; Carter et al., 1990; Pye, 1991; Erikson et al., 2007). Wave erosion along the seaward face of the dune may also initiate saucer-, cup- or trough-shaped depressions (Hesp, 2002). Based on this principle, Ruggiero et al. (2001) put forward a model designed to assess dune sensitivity to erosion generated by the impact of storm waves. This methodological approach was used for assessing vulnerability of barrier islands to hurricanes along the eastern coast of USA (Sallenger, 2000; Sallenger et al., 2004; Stockdon et al., 2007); it was also used for analysing decadal-scale variation in dune erosion and accretion rates on the Sefton coast in northwest England (Pye and Blott, 2008).

\* Corresponding author. Tel.: +33 2 98 49 86 10; fax: +33 2 98 49 87 03.

E-mail addresses: [serge.suanez@univ-brest.fr](mailto:serge.suanez@univ-brest.fr) (S. Suanez),[jean-marie.cariolet@univ-brest.fr](mailto:jean-marie.cariolet@univ-brest.fr) (J.-M. Cariolet), [romain.cancouet@univ-brest.fr](mailto:romain.cancouet@univ-brest.fr)(R. Cancouët), [fabrice.ardhuin@ifremer.fr](mailto:fabrice.ardhuin@ifremer.fr) (F. Ardhuin),[christophe.delacourt@univ-brest.fr](mailto:christophe.delacourt@univ-brest.fr) (C. Delacourt).

In contrast, even if processes of post-storm dune recovery are quite well known, few studies based on high frequency morphological and hydrodynamic survey have been undertaken on this topic. However, dune recovery offers the opportunity to test the interactions between climate and geomorphologic processes on relatively short timescales (Levin and Ben-Dor, 2004; Saye et al., 2005; Camacho-Valdéz et al., 2008; Claudino-Sales et al., 2008; Houser et al., 2008; Pye and Blott, 2008; Houser and Hamilton, 2009; Levin, 2011). The first study based on field observations concerns the model of dune recovery proposed by Carter et al. (1990). It deals with three phases associated with the undercutting, slumping and reforming of dune slopes. Therefore, the sediment removed from the dunes during scarping is usually returned to the slope face as part of the beach/dune recovery cycle. This process generally leads to echo dune formation due to initial sand accumulations between the mean high water springs (MHWS) and the scarp. Later, windblown material may accumulate at the crest, often in distinct lobes (Hesp, 1988), and/or on the mid-slope until the entire scarp is covered. Once the scarp slope is filled, and lying below the angle of repose, vegetation growth accelerates the dune recovery process. Nevertheless, the rebuilding of seaward faces does not mean that the dune front will have recovered its initial pre-storm position (Carter et al., 1990). This depends largely on shoreface–beach/dune sand exchanges which are determined by a wide range of environmental parameters, such as sand availability and wind conditions (Sherman and Bauer, 1993; Aagard et al., 2004; Anthony et al., 2006). More recently, Priestas and Fagherazzi (2010) studied dune recovery on Barrier Island in Florida after Hurricane Dennis (2005). They showed that overwash from the storm surge removed nearly the entire foredune but it was strongly dependant on dune morphology. Nevertheless, a year and a half after the hurricane, secondary dune recovery was still ongoing because of the large supply from beach to dune. However, it was shown by Houser and Hamilton (2009) on Santa Rosa Island (Florida) following Hurricane Katrina (September 2005) that beach morphological features control the supply to the dune. The authors showed that beach/dune system recovery occurred at the widest sections where overwash penetration was limited, leading to a large volume of sediment available for coastal system recovery. The effects of moisture have been also explicitly recognised in several studies to be a limiting factor because it increases threshold shear velocities and consequently reduces aeolian transport (Hotta et al., 1984; Namikas and Sherman, 1995; Sherman et al., 1998). In addition, on macrotidal beaches, surface moisture following tidal inundation may also delay initiation of transport by several hours, especially in the runnels, retarding optimum transport conditions even though wind speed and direction may favour for aeolian transport (Vanhée et al., 2002; Ruz and Meur-Ferec, 2004).

The aim of this study is to analyse dune recovery processes on Vougot Beach after Storm Johanna on 10th March 2008. In a previous study, the morphological impacts of this storm on Vougot Beach were analysed, as, when this event occurred, the beach had been undergoing morphological survey since July 2004 (Suanez and Cariolet, 2010). Therefore, in the present paper the objectives are: 1) to analyse and quantify morphosedimentary changes induced by dune recovery using ground observations and pre- and post-storm dune/beach morphological surveys; 2) to analyse hydrodynamic conditions by measuring and calculating extreme water levels – in this case, storm surge and swash run-up elevation based on tide and wave measurements; and 3) to produce a short to medium-term functioning scheme of the beach/dune system relative to dune recovery on Vougot Beach.

## 2. Geomorphological and hydrodynamic setting

The study area covers Vougot Beach located in the municipality of Guissény; it is situated on the north coast of Finistère in Brittany (Fig. 1). This coastal area comprises large rocky outcrops representing the submerged part of the Léon plateau. Contact between the coastal platform and the continental part of the plateau consists of a partly

tectonic scarp 30 m to 50 m high. In the Vougot Beach area, the scarp is disconnected from the sea due to the existence of a dune which was formed during the Holocene (Guilcher and Hallégouët, 1991). This dune, anchored on Zorn cliff, stretches over about 2 km in a southwest to northeast direction. It culminates at 13 m NGF in altitude (i.e. above sea level – asl). (The altimetric reference NGF – *Nivellement Général Français* – refers to French topographic datum. In our case this reference is situated 3.5 m above the spring-tide low-water level). It represents a massive dune complex 250 m to 400 m wide (Fig. 2a). The grain size of dune sand is about 200  $\mu\text{m}$ ; the sediment becomes coarser on the beach where grain size reaches 250 to 315  $\mu\text{m}$ .

Until the 19th century, this vast sand body was backed by wetlands which were connected to the sea in the Porz Olier sector located in the northeast. In 1834, a dike was built in order to isolate the area from the sea, and the wetlands were drained for agriculture. Today, this polder area, partly occupied by Curnic pond, stands near or below sea level. This low-lying land is also protected from the sea by the dune, which acts as a natural defence. This element is all the more important since this area is inhabited (camping, Curnic neighbourhood, farming, etc.).

Over the last decades, the dune of Vougot Beach has experienced erosion. A historical shoreline change analysis based on a series of aerial photographs and field measurements from 1952 to 2009 showed that retreat of the dune principally affected the eastern part of Vougot Beach (Suanez et al., 2010). Erosion was caused by the construction of the Enez Croas Hent jetty in 1974, which completely modified the hydrodynamics and interrupted the westward sand drift inducing an increase in sediment loss for the Vougot Beach/dune system. Calculation of erosion rates over the 1978–2000 period (following the building of the jetty in 1974) showed that the maximum retreat of the dune reached 0.6 m/yr; and this rate has increased from 0.6 m/yr to 1.5 m/yr over the last decade (from 2000 to 2009). However, the increase of dune retreat has to be qualified since the major erosion event related to the storm of 10th March 2008 occurred near the end of that period. This recent event probably contributes to the higher value which may not very representative.

The comparison between DEMs (Digital Elevation Models) obtained from the 2005 and 2009 surveys of Vougot Beach/dune system confirmed this evolution. A volume of eroded sand from the dune amounting to  $-10,677 \pm 72 \text{ m}^3$ , together with an erosion of the foreshore beach of  $-10,933 \pm 931 \text{ m}^3$ , was determined (Suanez et al., 2010). Most of this material was transported to the west and contributed to building-up the western section of Vougot Beach, which gained  $4,505 \pm 489 \text{ m}^3$ . This longshore sand transport is due to wave diffraction generated by small islands and reefs, such as Enez Du, situated on the tidal zone (Fig. 2a).

The macrotidal range, reaching 8.5 m, is responsible for the large tidal beach surface which can be exposed over more than 400 m at low tide. The deep-sea wave characteristics are presented on wave rose in Fig. 2a. These wave data have been calculated by numerical run model over the period 1979–2002 at the location point off Vougot Beach at 64 m water depth ( $4^{\circ}50'10''\text{W}$  and  $48^{\circ}44'30''\text{N}$ ) (Fig. 1a). The principal offshore waves arriving in the Guissény area mostly come from a west-northwest direction (Fig. 2a). Their modal height ( $H_{\text{mo}}$ ) is between 1 and 1.5 m, and the modal period ( $T_{\text{pic}}$ ) between 9 and 10 s. The Guissény shoreline is relatively well protected from west to northwest waves by the platform scattered with islets and reefs emerging at low tide (such as Golhédoc or Enez Du). These features complicate hydrosedimentary flows at the coast, generating major diffraction phenomena which account for the many 'comet tails' formed in the lee of these obstacles (Fig. 2a). It is also these islets and reefs that give the dune line its convex curved shape by sheltering the coast. Nearshore wave deformation is also expressed by a local westward coastal drift, as is the case at the beach of Centre Nautique and on the eastern section of Vougot Beach (Fig. 2b). Wind velocity and directional frequency data were obtained from the

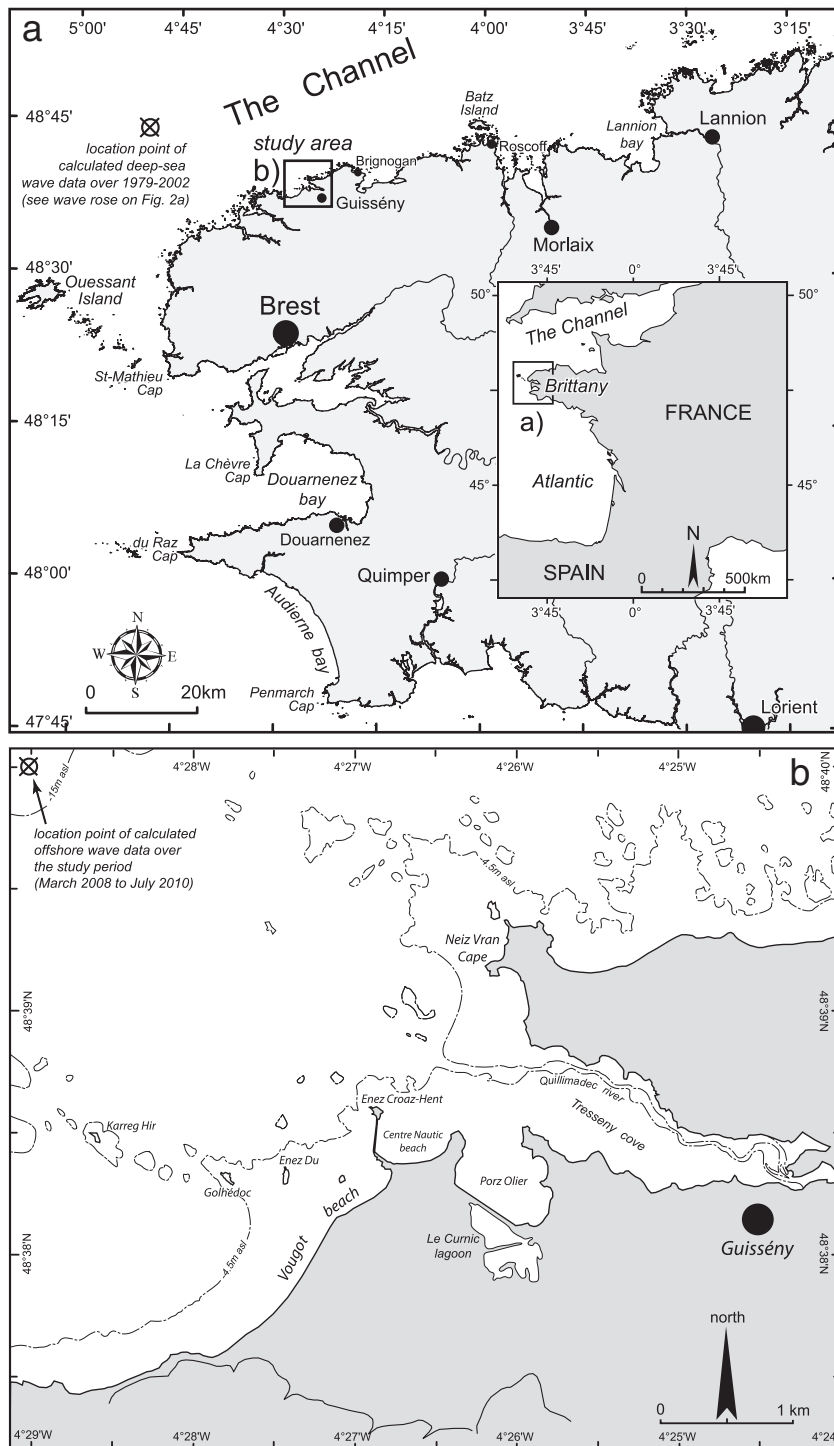


**Fig. 1.** The general location (a), Vougout Beach (b).

nearest meteorological station run by Météo France at Brignogan. The most frequent annual winds are from west-southwest with a moderate north-eastern component (Fig. 2a). The seasonal variations of these meteorological and marine components are presented in Fig. 3. The winter period (December to February) is characterised by strong winds ( $> 8$  m/s for more than 30%) blowing from northwest to southwest. These winds are associated with west-northwest waves (96%). Wave heights and periods associated with storm events are the strongest (respectively  $\geq 10$  m and 18 s for the largest storms). During spring (March to May), waves are less energetic (36% of wave heights reached 2 to 4 m and 34% of wave periods 8 to 12 s) while the northeast

wind direction increases (20%). The summer period (June to August) is characterised by significant low energy marine conditions. During the autumn (September to November), again energetic conditions increase close to the winter period. Dominant winds are from northwest to southwest (35%) and wave parameters are reinforced.

### 3. Impact of the storm of 10th March 2008 on dune erosion

On 10th March 2008, a severe storm hit western France, causing major damage on the coasts of Brittany and Normandy. From a geomorphological point of view, the erosive effects induced by this storm were



**Fig. 2.** a) Geomorphological map: 1: wave-cut platform. 2: island. 3: gravel sheet. 4: sand beach. 5: mud flat. 6: outer dune. 7: inner dune. 8: sandy-silt deposit. 9: silt. 10: brackish marsh. 11: river. 12: dune scarp. 13: rocky cliff. 14: periglacial cliff. 15: abandoned cliff. 16: comet tail. 17: drift current. 18: wave refraction. 19: sea defence structure. 20: fault. 21: urban zone. Wave rose established from data obtained by a numerical model over the period 1979–2002 (source: Laboratoire National d'Hydraulique et d'Environnement, LNHE-EDF Chatou, and Centre d'Etudes Techniques Maritimes Et Fluviales, CETMEF-Brest). Wind rose established from data obtained by the Météo France record station at Brignogan over the period 1984–2007. b) Aerial photograph taken on 14 August 1978 during high tide. This photo shows wave refraction–diffraction around islets inducing a main sediment transport from east (transects 1 and 2) to west (transect 3) — see arrows 1, 2 and 3. Even if front of transect 3 sediment transport is oriented from west to east (see arrow 4), we suggest that the net longshore sediment transport in the study area is oriented from east to west according to the angle  $\alpha$  given by last wave crests on the shoreline.

not associated with exceptionally energetic waves (2-year return period interval), but rather with the fact that the storm was combined with a high spring tide (Cariolet et al., 2010). The extreme water levels at the coast exceeded the altitude of the dune toe on Vougot Beach by several metres, causing severe erosion (Suanez and Cariolet, 2010). The maximum retreat reaches around 6 m (Fig. 4a).

Similarly, dune/upper intertidal beach profile measurements taken along three transects also showed significant dune retreat (Fig. 4b, c,d). Calculations of sediment budget performed for both sections of profile showed that for transects 1 and 2 the quantity of sediment lost through dune retreat (respectively  $-9.1$  and  $-8.51 \text{ m}^3 \cdot \text{m}^{-1}$ ) was counterbalanced by a sediment gain on the upper intertidal zone

(respectively  $+10.24$  and  $+16.45 \text{ m}^3 \cdot \text{m}^{-1}$ ) (Fig. 4b,c). On the other hand, the results obtained for transect 3 (Fig. 4d) showed that the entire dune/upper tidal beach profile had undergone erosion. These morpho-sedimentary processes showed that the adjustment principle of the equilibrium profile described by Dean (1991) between the dune and the upper tidal beach zones functioned correctly on the eastern part of Vougot Beach. Further west, the longshore sediment transport disturbed cross-shore transfer between the dune and the beach (Suanez and Cariolet, 2010).

#### 4. Methods and data analysis

##### 4.1. Morphological survey

An aerial and tidal beach survey was carried out using a Trimble 5700/5800 Differential GPS. Data points described by three coordinate values ( $x, y, z$ ) were collected in Real Time Kinematic (RTK) mode. Each DGPS measurement was calibrated using the geodesic marker from the French datum and the geodesic network provided by the IGN (*Institut Géographique National*) located about 2 km from the study area. Five control points were defined in the field to assess the accuracy of the surveys. Since the beginning of the survey, about 100 field campaigns have been carried out. For each of them, the position of the control points was measured and the margin of error for the three dimensions ( $x, y$ , and  $z$ ) was calculated using standard deviation. The results show an  $x, y, z$  accuracy reaching, respectively, 4–5 cm ( $x$  and  $y$ ) and 1 cm ( $z$ ). These values were used to calculate the margin of error associated with the sediment budget calculation. The first survey consisted of annual foredune change measurements

using the edge of the dune as the erosion reference feature (ERF). This limit is highly relevant because it corresponds to the top of the bluff cut by erosion processes, which clearly demarcates the dune vegetation from the loose sand of the backshore (Crowell et al., 1991; Zuzek et al., 2003).

The second survey was based on a detailed monitoring of the tidal beach/dune surface changes. This morphological measurement was carried out using the same method as that used for both similar surveys conducted in 2005 and 2008–2009 (Suanez et al., 2010). The survey took place from 12th to 15th July 2010. It was carried out only on the tidal beaches and the loose sand close to the dune bluff contact. Vegetated dunes, skerries, and small islands showing no changes were not monitored any further. These invariable points from the first survey in 2005 were used. Surfer 8.0 software was used to import and process the ( $x, y, z$ ) data. A kriging interpolation model supporting breaklines was applied to convert data point observations into continuous field grids (altitude matrices). The whole study area contour lines and 3D visualisation were generated from a 0.5 m grid. Morphological changes were analysed by calculating the volumetric difference between both surfaces from November 2008–January 2009 and July 2010.

The third survey consisted of the continuation of beach/dune profile measurements carried out along the three cross-shore transects presented in Fig. 4e. Measurements continued to be carried out once a month, which represents the frequency established since the survey started in July 2004 (Suanez and Cariolet, 2010). Quantification of sediment budgets based on the 'vertical surface calculation' method was performed on two different sections of the profile: the upper tidal beach and the dune defined by the slope steep face.

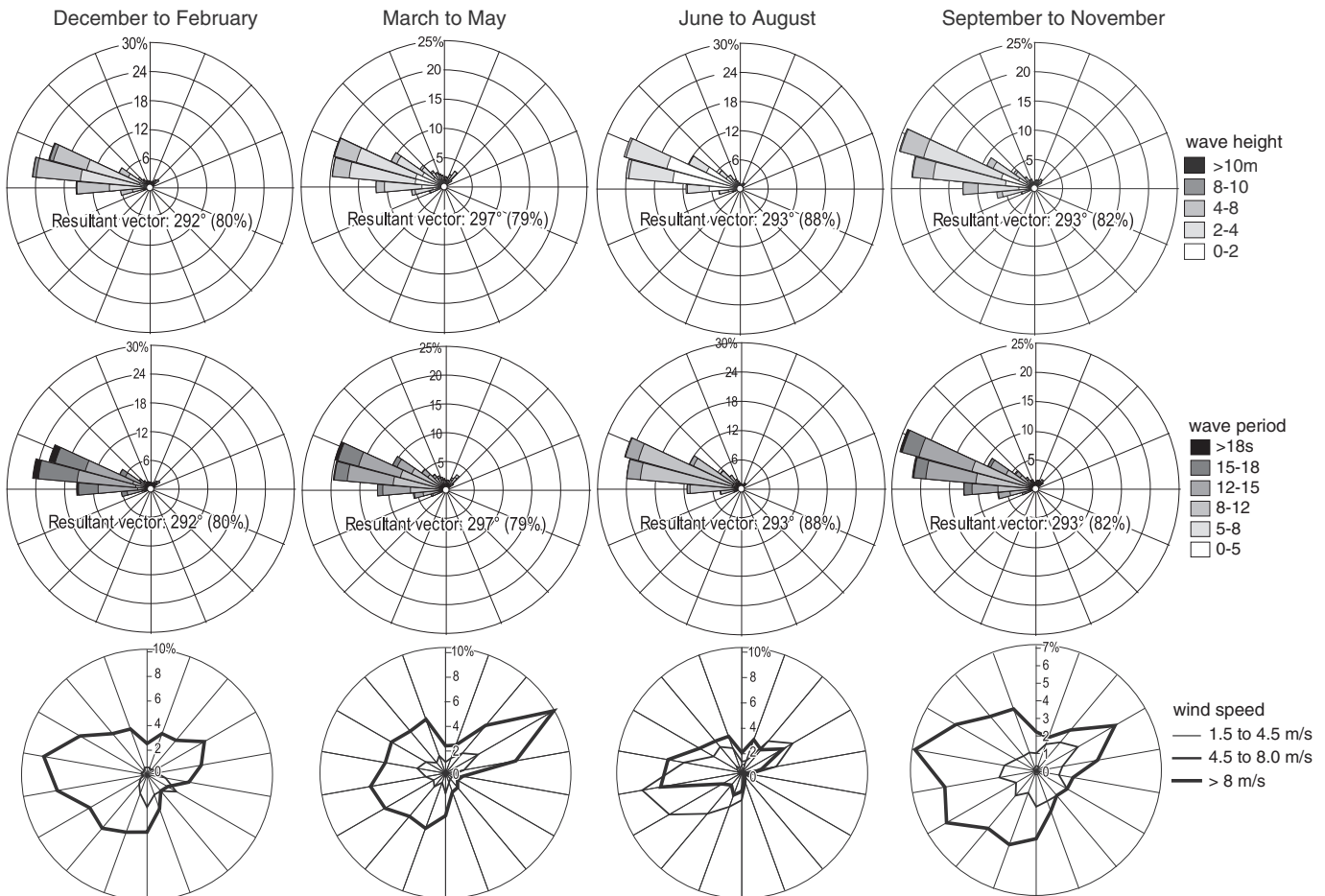
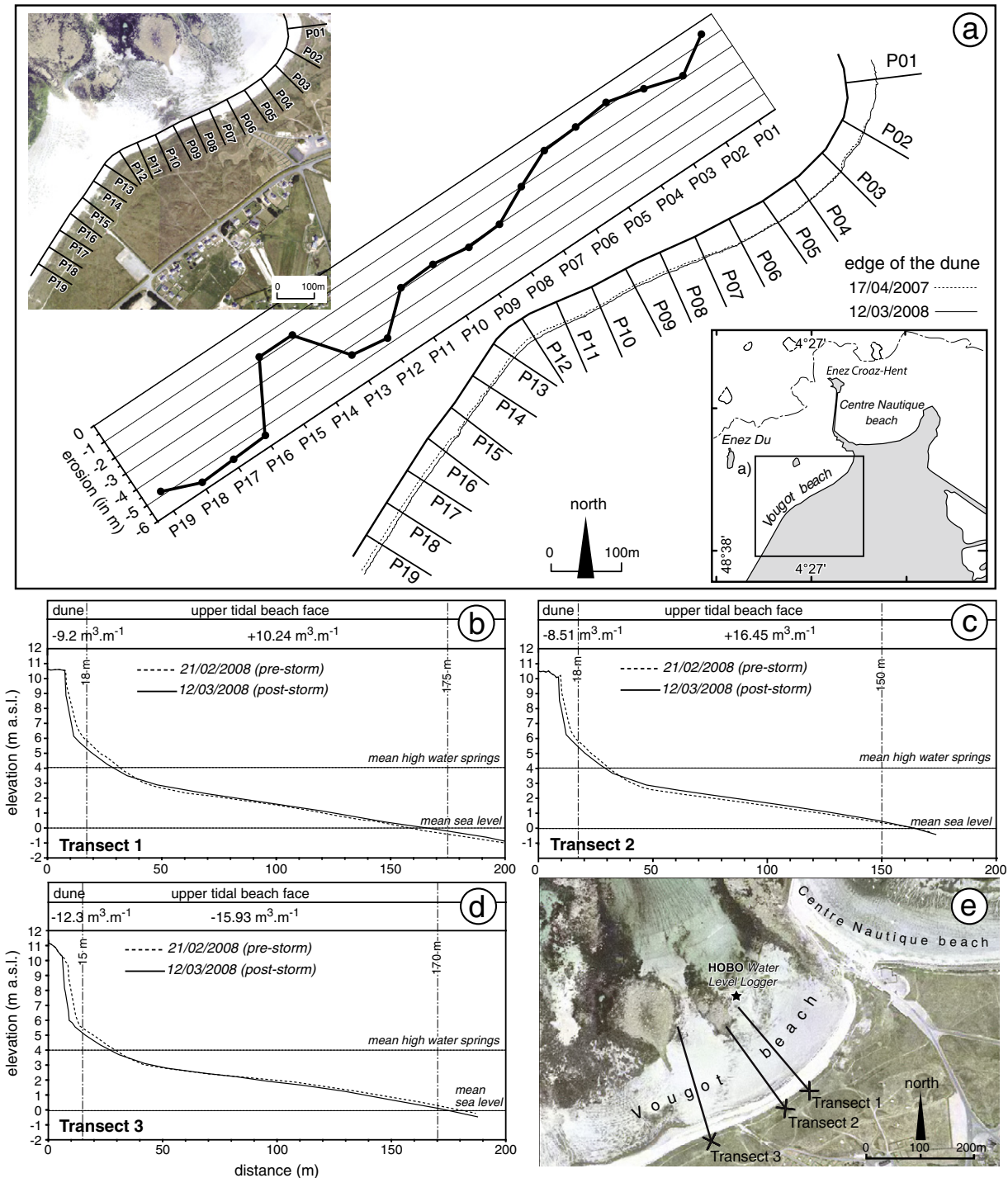


Fig. 3. Seasonal variations in wave and wind components.



**Fig. 4.** Foredune erosion of Vougot Beach obtained by field measurements two days after the 10th of March storm. a) Dune front retreat (no data concerning the 2007 position of the front of the dune was available further than profile P19). b), c) and d) Beach/dune profile measurements taken before and after the storm of 10 March 2008. Sediment budgets mentioned at the top of the graphs were calculated for two different sections of the profile (the dune and the upper beach face), delimited in terms of distance by metric values mentioned on the envelope of profiles (according to Suarez and Cariolet, 2010).

Finally, a bathymetric survey was conducted on 29th July 2010 so as to analyse the seabed morphology beyond the low spring tide level. An area where DGPS terrestrial topographic measurements overlap these bathymetric measurements (see Fig. 16) was used to control the quality and consistency of bathymetric measurements. These bathymetric measurements were achieved using a high resolution, shallow water multi-beam echo sounder (MBES) (RESON SeaBat 8101) operating at 240 kHz. It was positioned using two bi-frequency GPS receivers (SEPTENTRIO) functioning in RTK mode,

while the mobile installed on the boat received the differential corrections from the base set up near the sailing school beach via a UHF radio link. Navigational accuracy was estimated at  $\pm 2$  cm horizontally and  $\pm 4$  cm vertically. The vessel's movements (roll, pitch and heading) were measured by a motion sensor (iXSea OCTANS) submerged near the echo sounder head. Several velocity profiles were obtained in the survey area to control the sound propagation speed in water. Complete calibration of the MBES system was performed before the survey by applying the standard procedures in

operation. The bathymetric data were processed using the specialised software QINSy 8.00 and included: integration and synchronisation of echo sounder data with that of related sensors, navigation control, correction of systematic errors (velocity, calibration) and cleaning of erroneous sensors. A georeferenced DEM (Digital Elevation Model) with a grid size of 0.5 m was produced and integrated with the existing topographical dataset.

#### 4.2. Hydrodynamic condition analysis

The hydrodynamic conditions were analysed to assess the sensitivity of the dune to extreme water levels by applying the “Property Erosion Model” method by Ruggiero et al. (2001). The extreme water levels were calculated using the two parameters affecting water elevation at the coast: storm surge (obtained from the measured tide) and run-up (combined effects of set-up and swash run-up generated by swell).

Measured tide data were obtained from the Roscoff tide gauge station located at about 30 km from the survey area (Fig. 1a). So as to correct the site effects related to the large distance between Roscoff and Guissény, a HOBO U20 Water Level Logger-Onset® was used to record the water levels between November 2009 and March 2010 on Vougot Beach (Fig. 5a). It was set up on a rocky outcrop located in the middle of the upper tidal beach to the right of transect 1 (Fig. 4e). A recording frequency of 2 min was used and the data were smoothed to a moving average of 10 to filter out deformations of the water surface related to wave action. The maximum daily water level was extracted for each of the two series from the Roscoff tide gauge station and the HOBO logger, so as to only work on high tide levels. The correlation between these daily high tide levels measured on Vougot Beach and in Roscoff show a difference of  $13 \pm 2$  cm (Fig. 5b,c). A similar result of about 0.20 m was obtained by the SHOM (*Service Hydrographique et Océanographique de la Marine* – French Army) concerning the difference of extreme water level of 100-year return period between Roscoff (where tide gauge record is set up) and our study area (SHOM-CETMEF, 2008). The value of 0.13 m was taken to correct the tidal data from Roscoff, recorded for the entire observation period (April 2008 to July 2010).

Run-up was calculated via a semi-theoretical approach using the basic equations established by Hunt (1959), Battjes (1971) and Holman (1986). These equations draw upon the relationship between the maximum vertical elevation of run-up and two additional factors which are the offshore wave height  $H_o$  and the Iribarren number (or surf similarity parameter) which itself includes the beach slope  $\tan\beta$ :

$$\frac{R^T}{H_o} = C\xi_o \quad (1)$$

where  $R^T$  is the value of the run-up, which is the sum of set-up and swash ( $R^T = \bar{\eta} \max + R$ );  $H_o$  is the significant wave height (in metres);  $C$  is a dimensionless constant; and  $\xi_o$  is the Iribarren number (Battjes, 1974):

$$\xi_o = \frac{\tan\beta}{(H_o/L_o)^{1/2}} \quad (2)$$

where  $H_o$  is the offshore wave height (in metres);  $L_o$  is the wavelength (in metres); and  $\tan\beta$  is the beach slope.

In our case, one of the difficulties lay in using these formulas which were established from in situ measurements on micro- to mesotidal beaches. The slope values generally used therefore represent the slope of the foreshore (Holman and Sallenger, 1985; Nielsen and Hanslow, 1991; Stockdon et al., 2006). However, in a recent study based on measurements of watermarks as an indicator of the limit of run-up, Cariolet (2011a) showed that in a macrotidal context, the slope of the active section of the upper beach was more

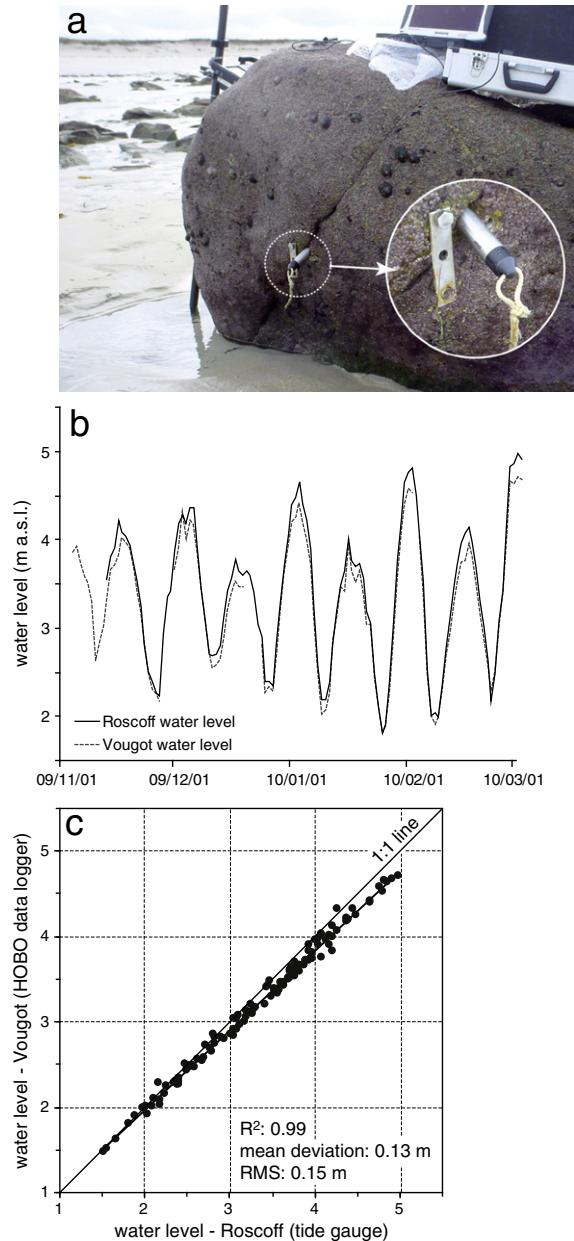


Fig. 5. Comparison between daily high tide water level recorded at Vougot Beach using the Hobo data logger and at Roscoff using the tide gauge record.

appropriate for the use of these formulas. By applying the same semi-theoretical approach based on field measurements, a formula was calibrated for Vougot Beach (Cariolet, 2011b). This formula shows once again that the slope of the active section of the upper beach gives the best adjustments when compared with the results obtained in terms of maximum swash height, with in situ measurements of the watermarks indicating the limit of wave swash (Fig. 6):

$$R_{\max} = 0,7H_o\xi_o \quad (3)$$

where,  $R_{\max}$  is the run-up;  $\tan\beta$  is the slope of the moving section of the upper beach; and  $H_o$  and  $L_o$  are offshore wave height and wavelength. The offshore wave data used to calculate run-up between March 2008 and July 2010 were acquired by modelling using the digital model WAVEWATCH III™ (Ardhuin et al., 2009, 2010), at the calculation point  $4^{\circ}29'24''$  W,  $48^{\circ}40'12''$  N in 18.3 m water depth (Fig. 1b).

4.3. Meteorological conditions and aeolian transport

The analysis of meteorological conditions was based on the acquisition of wind and rain data recorded for the entire observation period by the Météo France station in Brignogan located around 15 km from Vougot Beach (Fig. 1a). The aim was to investigate whether dune growth was correlated with specific wind conditions, considering that the Vougot dune, oriented 60°N-240°S, is influenced by both main wind directions of west and northeast (Fig. 3). Morphogenetic winds were only considered when the measured speed  $V^*$  was greater than the critical shear velocity  $V_c^*$  calculated from the Bagnold (1941) formula:

$$V_c^* = k_1 [(\rho_s/\rho_a)(gd)]^{0.5} \tag{4}$$

where  $k_1$  is a constant = 0.1;  $\rho_s$  is sand density (2.7 g/cm<sup>3</sup>);  $\rho_a$  is air density (0.0023 g/cm<sup>3</sup>);  $d$  is mean grain diameter in cm; and  $g$  is gravitational acceleration (9.81 m/s<sup>2</sup>).

For an average grain size of 200 to 250 μm, constituting the mobile sands of the dune/upper beach system, the critical shear velocity  $V_c^*$  was between 4.7 and 5.4 m/s. A threshold of between 5.0 and 5.5 m/s was chosen to filter raw data for wind data analysis.

5. Results

5.1. Morphological changes

The evolution of the dune front since the 10th March 2008 storm shows that the maximum retreat reached -1.4 m in two years, i.e. approximately 0.7 m/year (Fig. 7). This value is similar to that obtained through the study of the kinematics of the dune edge over the period 1978-2000 (Suarez et al., 2010).

Analysis of beach profile measurements shows that since the storm on 10th March 2008, the upper tidal beach/dune system has changed considerably. Generally speaking, severe erosion of the upper tidal beach (≥1 m depending on the sectors) can be observed, while the upper part of the upper tidal beach and the dune toe accreted (Fig. 8). Erosion of the upper tidal beach led to the almost complete disappearance of a sand sheet, revealing an irregular topography comprising outcrops of organic-rich freshwater peat layers, and/or periglacial deposits such as head, and/or Pleistocene shingle accumulations (Fig. 9). Accretion of the upper beach (especially the backshore above MHWL) and dune toe led to the construction of embryo dunes reaching 1 m high and forming a secondary line of dunes. Nevertheless, in the details, these results show that transects 1 and 2 functioned similarly, while the evolution of transect 3, located further west, differs from the first two.

The analysis of the sediment budget achieved for the two profile sections – the upper tidal beach and the dune – between April 2008 and July 2010, shows that the upper tidal beach/dune system at transects 1 and 2 functioned in a similar way. Continuous and regular supplying of the dune toe was observed over the whole period of survey ( $r^2$  between 0.93 and 0.97) inducing a readjustment of sediment budget (Fig. 10). Therefore, the volume of sediment lost by the dune during the storm of 10th March 2008 for these two transects – as we mentioned above, respectively -9.2 and -8.5 m<sup>3</sup>.m<sup>-1</sup> (Fig. 4b, c) – has almost entirely recovered (respectively +8 and +7.75 m<sup>3</sup>.m<sup>-1</sup> for transects 1 and 2). On the other hand, continuous and regular erosion ( $r^2$  between 0.88 and 0.78) was observed for the upper tidal beach; this loss of sediment reaches, respectively, -47.6 and -42 m<sup>3</sup>.m<sup>-1</sup> for both transects 1 and 2 (Fig. 10). In detail, this erosion proved to occur very rapidly; the survey in April 2008, just one month after the storm, showed that the upper tidal beach lost between -9.5 and -10 m<sup>3</sup>.m<sup>-1</sup> at transects 1 and 2. As we shall see below, this evolution could be the result of very rapid post-storm processes operating to readjust the equilibrium beach profile, as explained by Dean (1991).

At transect 3, sediment budget evolution shows different behaviour, whereby the entire upper tidal beach/dune system accreted. For the whole period of survey, a regular sediment volume gain ( $r^2$  0.92), reaching +5.3 m<sup>3</sup>.m<sup>-1</sup>, was recorded for the dune. However, this volume remains lower than that lost by this same sector during the storm of 10th March 2008 (-12.3 m<sup>3</sup>.m<sup>-1</sup>, see Fig. 4d). Similarly, a sediment volume gain reaching +11.5 m<sup>3</sup>.m<sup>-1</sup> was recorded for the upper tidal beach, which is almost equivalent to the volume lost on the 10th March 2008 (-15.9 m<sup>3</sup>.m<sup>-1</sup>, see Fig. 4d). However, when analysed in detail, this sediment supply proves to have been highly irregular ( $r^2$  0.01). After a major supplying phase between April 2008 and August 2009, a significant sediment loss phase was observed.

The topographic survey based on comparison between DEMs obtained from the November 2008-January 2009 and July 2010 measurements confirms this evolution. Calculation of the sediment budget and construction of sediment transport using the 'box model' method, show that the entire dune and the upper beach accreted by +1,816 ± 141 m<sup>3</sup> and +11,934 ± 928 m<sup>3</sup>, respectively (Fig. 11). This positive sediment budget was recorded in spite of the 0.4 to 0.7 m/year post-storm dune edge retreat. This erosion is largely associated with dune collapse and/or slides accompanying post-storm dune profile readjustment phenomena (Carter et al., 1990). Dune accretion occurred principally at the dune toe and led to the construction of embryo dunes (Fig. 12a-e). Locally, as described by Hesp (1988), wind blown sand accumulated on the crest, generating small lobes, and on the mid-slope inducing accretion on the entire

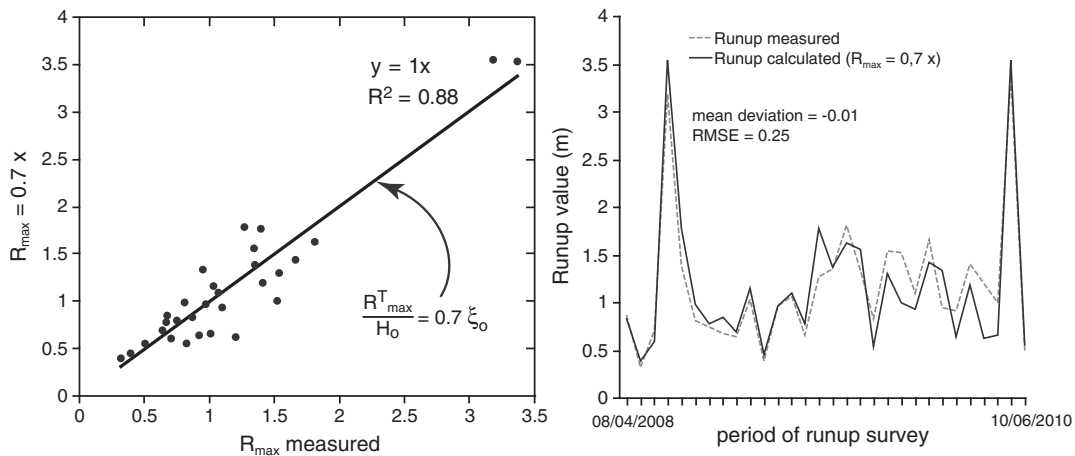
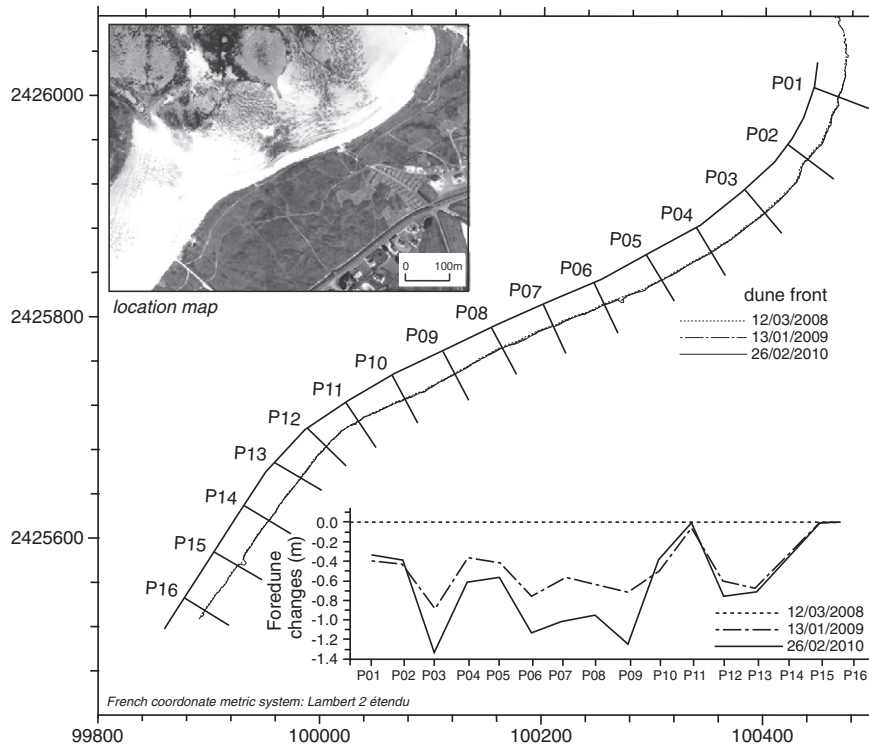


Fig. 6. Measurements of the maximum run-up at Vougot Beach. The measured run-up was normalised to the 0.7 constant and compared with the calculated run-up given by Eq. (3).



**Fig. 7.** Foredune changes (m) at Vougot Beach obtained by DGPS field measurements for 2008, 2009 and 2010.

scarp (Fig. 13). On the other hand, the upper tidal beach lost  $-23,857 \pm 2,302 \text{ m}^3$ . This evolution confirms the results obtained by the analysis of beach profile measurements (Fig. 8). However, calculation of the overall sediment budget for the entire study area showed a deficit of around  $10,000 \text{ m}^3$ , in spite of the low accretion recorded at the low tide terrace (Fig. 11).

5.2. Role of hydrodynamic and meteorological conditions

Analysis of hydrodynamic conditions, as previously indicated, is based on the estimation of extreme water levels at the coast. This information was combined with the height of the dune toe measured along the three transects. The maximum water levels obtained for

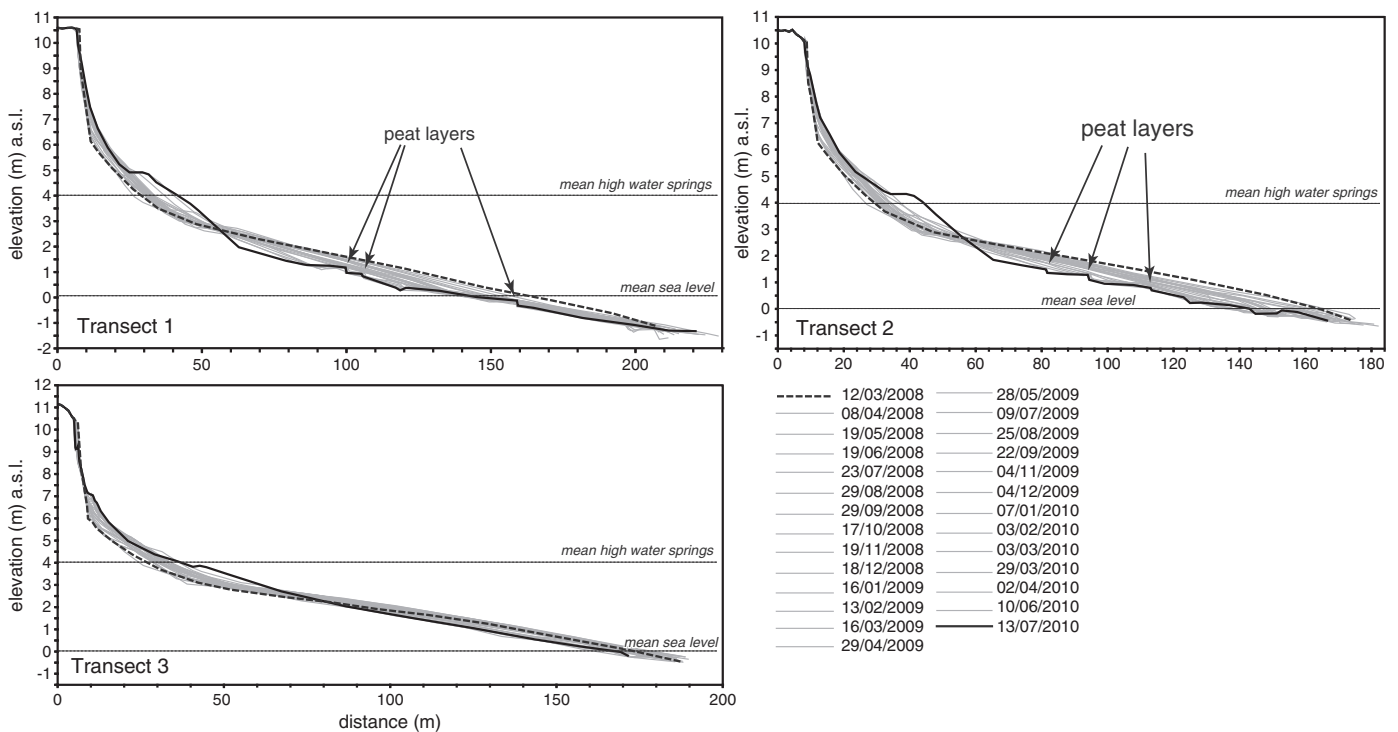


**Fig. 8.** Intertidal beach/dune profile changes for transect 1, 2 and 3 from 12 April 2008 to 13 July 2010.



**Fig. 9.** Pre and post-storm morphosedimentary setting of the upper tidal beach of Vougot. a) Pre-storm morphosedimentary setting of the upper beach on 10/09/2007 when sand sheet was present. b) Immediate post-storm morphosedimentary setting on 20/05/2008 when sand sheet was still present. c) and d) respectively 1.5 and 2.5 years post-storm morphosedimentary setting showing an outcrop of peat layers and periglacial deposits on the upper beach due to the erosion of the sand sheet (photos: CEVA – Pleubian).

the storm of 10th March 2008 reach over 10 m asl, i.e. more than 4 m above the dune toe (Fig. 14). This extreme water level calculation is in accordance with field observations made the day of the storm. As shown in Fig. 12b, during the p.m. high tide, the highest swash run-up reached the dune crest. After the storm of 10th March 2008, the water levels calculated for the whole survey period exceeded the dune toe elevation six times during which the dune did not erode; between December 2008 and January 2009, between October and December 2009 and at the end of March 2010 (Fig. 14). This is mainly due to the fact that these high water levels were not sufficiently energetic to have a real effect on the erosion of the dune toe where

accretion continued. This could also be explained by the fact that morphological measurements were rarely achieved just after high water level events. Therefore, if the erosion phase was not so important, a few days marked by aeolian sediment supply to the dune were sufficient enough to make the dune sediment budget positive and/or stable, instead of eroding. This sediment supply was all the more efficient as the dune retreat created accommodation space suitable for accretion.

The relationship between the evolution of the dune sediment budget and meteorological conditions did not reveal any particular link (Fig. 15). Dune accretion, which was similar for the three transects, occurred in five more or less marked phases (Fig. 15a). While the second and fourth were associated with high wind speeds ( $\geq 20 \text{ m.s}^{-1}$ ), this seems to be less the case for the three others (Fig. 15b). Similarly, there is no marked relationship between dune accretion and wind direction (Fig. 15c). Phases 1 and 3, concentrated during the summer, were associated with predominantly westerly winds confirming the observations made above on seasonal wind variation (see Fig. 3). The three other phases, mainly concentrated during the winter, were more marked by alternating westerly and north-easterly winds. This was particularly the case during the winters of 2008–2008 and 2009–2010 when long periods of anticyclonic conditions associated with NE winds alternated with periods of cyclonic storminess associated with westerly winds. The last factor, characterised by rain, showed no clear relationship with the evolution of the dune sediment budget either (Fig. 15d). For example, during the particularly damp phase 4, dune accretion was as high as during the final phase in which rainfall was very low.

Statistical analysis was achieved in order to describe the relationships between environmental variables and dune sediment budget changes (Fig. 16). The first correlation between sediment budget and wind speed indicates a relatively weak relationship ( $r^2$  between 29% and 30%). However, in terms of aeolian dynamic processes this relationship is consistent as the more the wind speed increases, the greater is the volume of sediment transferred. The statistical analysis of the relationships between sediment budget and rainfall and wind direction offer a very poor degree of correlation (respectively,  $r^2$  between 1% and 12%, and  $r^2$  between 0.5% and 10%). This is mainly due to the fact that the beach is a complex non-linear system and morphological change can rarely be explained by the variability of one driver in isolation. However, the positive yet weak correlation between the sediment budget and rainfall could be explained by the fact that the strongest winds are blowing from the west (see Figs. 2a and 3) and are generally associated with Atlantic stormy and rainy conditions. The correlation between wind direction and sediment budget could also indicate that from the eastern part (transect 1) to the western part (transect 3) of Vougot dune, the processes differ. Dune accretion in the eastern part is linked more to westerly winds, while in the western part it is promoted more by NE winds. This can be explained by the fact that the jetty at Carnic protects the eastern part of the beach from E to NE winds, while only W winds can supply sediment to the dune in this area. The further west you go, the less this sheltering effect occurs; NE winds may therefore be far more efficient in aeolian transport.

The last element of analysis between dune erosion phases and the previously calculated extreme water levels (Fig. 14) does not show any relationship either. With the exception of two erosive phases on 16th January 2009 and 10th April 2010, that can be linked to high water levels on 12th January 2009 and 31st March 2010, respectively, none of the other erosion phases match extreme water levels at the coast. This shows that dune crest retreat during this major period of foredune recovery was not linked to undercutting of the dune toe. This is also confirmed by the continuous rise of the dune toe along the three transects (Fig. 14). These few phases of erosion are, as seen above, the result of spasmodic dune crest retreat due to slumping phenomena, which continued for the two and a half year observation period at a relatively low rate (Fig. 7).

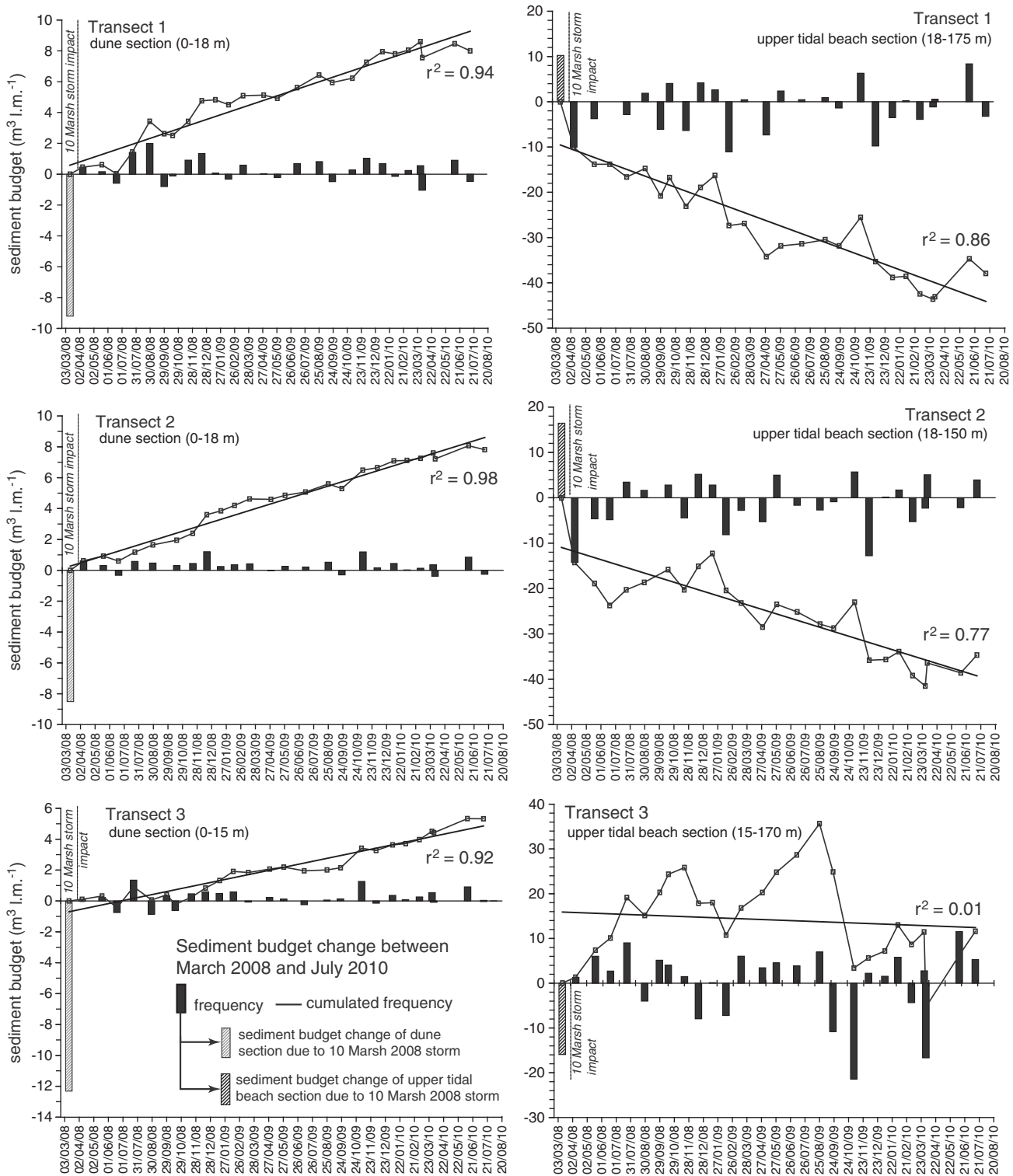


Fig. 10. Sediment budget evolution on two section of beach profile (dune and upper beach section) for transects 1, 2 and 3, between March 2008 and July 2010.

## 6. Discussion

As many previous studies have shown, post-storm dune recovery processes on Vougot Beach are principally the result of sediment transfer between the tidal beach and the dune toe. This sediment supply allowed the restoration of dune sediment budget equilibrium, without however promoting progradation of scarp slope filled to the initial pre-storm position. Nevertheless, as described by Carter et al. (1990), the rebuilding of the seaward dune face tended to maintain

the pre-storm dune form, particularly on well-vegetated slopes. This sediment supply also led to construction of sand accumulations forming embryo dunes between the high water level and the scarp, i.e. in the accommodation space resulting from the several metres retreat of the dune toe during the 10th March 2008 storm. Later sediment storage induced the elevation of this space. This process tended to reduce storm surge impacts and increase dune toe/upper beach accretion.

Budget calculation showed that the sediment volume lost from the upper tidal beach over the 2.5-year period was far greater than

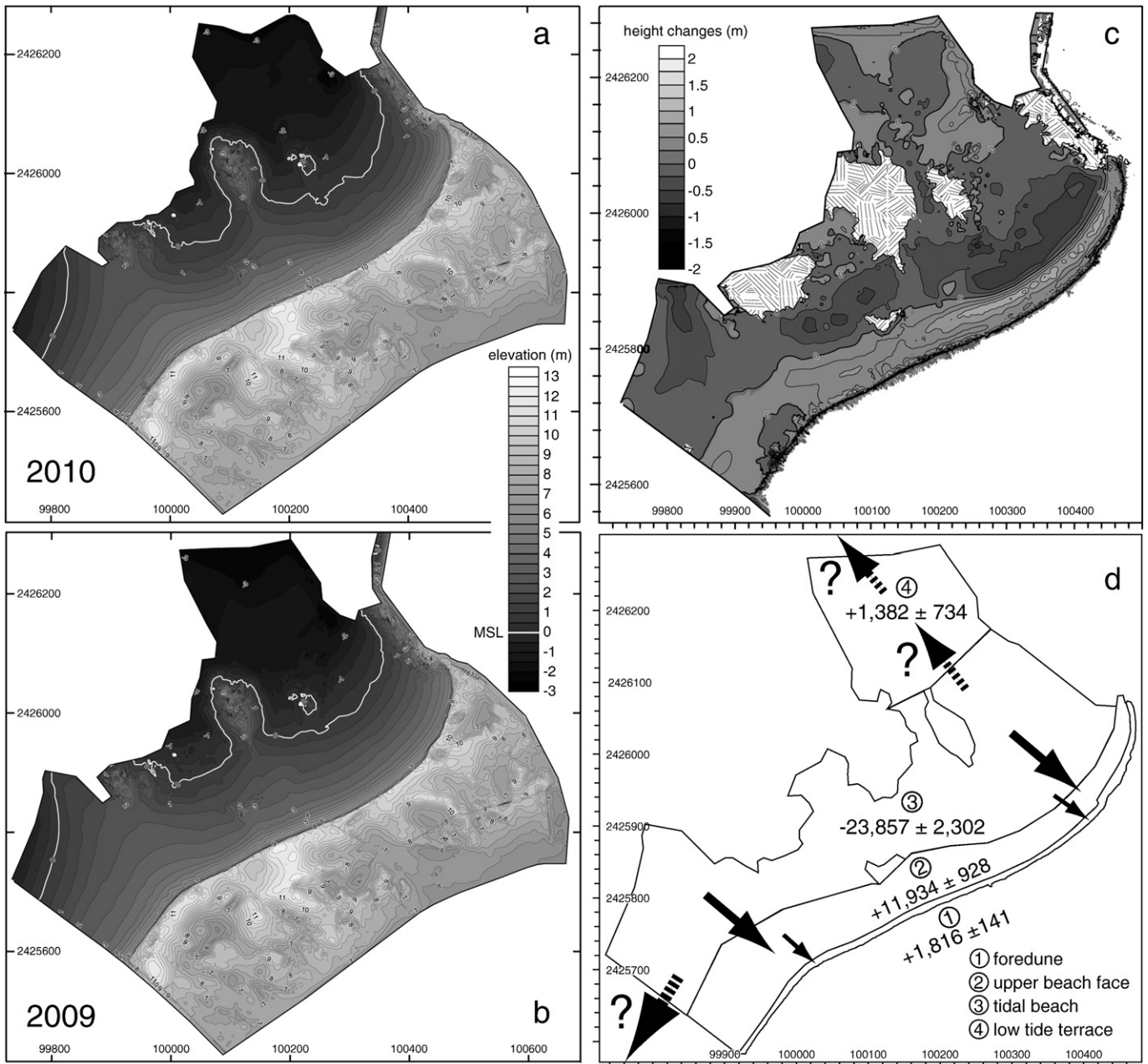


**Fig. 11.** 2010 (a) and 2009 (b) Digital Elevation Model. c) Altimetry differences between the 2009 and the 2010 DEMs. d) Box model illustrating sediment transport (values given in  $m^3$ ).

that gained by the dune. The topographic measurements achieved between November 2008–January 2009 and July 2010 show a loss of  $10,000 m^3$ ; this is confirmed by the beach profile measurements which indicate that at transects 1 and 2, the upper tidal beach lost, respectively  $-38$  and  $-35 m^3.m^{-1}$ , while dune accretion represented only  $+8$  and  $+7.8 m^3.m^{-1}$ . On the other hand, for the third transect located further west, the entire upper tidal beach/dune system accreted. These results prompt us to put forward two hypotheses on the morphosedimentary functioning which operates alongside dune recovery processes.

1 – The sediment deficit of the eastern part of Vougot upper tidal beach could be explained by sediment transfer from east to west (Fig. 11). This type of transfer was previously observed between 2005 and 2009 (Suarez et al., 2010). It is associated with a longshore hydrosedimentary drift from east to west, induced by wave refraction–diffraction phenomena around the islets and/

or reefs located seaward of the shoreline (Fig. 2b). It is also associated with aeolian transfer generated by east to northeast winds which, as seen above, represent a non-negligible proportion of the annual wind regime in this sector (Figs. 2a and 3).

2 – Sediment deficit could also be related to phenomena involved in restoring an equilibrium beach profile between the tidal beach and the nearshore to shoreface zone. As demonstrated by several authors, severe storms are often accompanied by offshore currents such as seaward return currents, generating major cross-shore seaward sediment flows (Winant, 1980; Snedden et al., 1988; Bradshaw et al., 1991; Wright et al., 1991; Héquette and Hill, 1993). This sediment transport is often the cause of severe offshore beach erosion which can reach great depths (Gayer, 1991; Héquette and Hill, 1995; Lee et al., 1998). Recent work achieved by Lentz et al. (2008) showed that onshore volume transport due to surface gravity waves propagating toward the beach can result in a compensating offshore flow referred to as



**Fig. 12.** Morphosedimentary changes of the dune over the past two and a half years. a) pre-storm dune morphology showing gentle slope face partially vegetalised b) Storm surge and wave attack on dune front during the 10 March 2008 storm. c) Vertical scarp, slumps and failures affecting post-storm dune slope profile. d) e) and f) Supply of dune toe leading to the construction of embryo dunes. These embryo dunes were colonised and stabilised by four main plant species: *Cakile maritime*, *Atriplex laciniata*, *Salsola kali*, *Elymus farctus*.



**Fig. 13.** Construction of lobes at the crest dune due to windblow material accumulation.

undertow in the shallow water, for instance in the surf zone. The authors mentioned that these observed offshore flows indicated that wave-driven seaward return currents extend well offshore of the surf zone, over the inner shelf. The monitoring conducted for this study was unable to measure these morphosedimentary dynamics as measurements were limited to the intertidal beach. However, the bathymetric survey conducted in July 2010 showed sediment features perpendicular to the shore at depth up to  $-12$  m asl (Fig. 17). These features could have been formed by cross-shore sediment transport induced by seaward return currents.

Beach profile readjustment following these erosion phenomena on the nearshore to shoreface zone would therefore result in post-storm sediment transport between the upper tidal beach and the lower tidal beach-nearshore to shoreface zone. These processes have been particularly well described by Dean (1991) but also by Lee et al. (1998) in the frame of the Field Research Facility (FRF) at

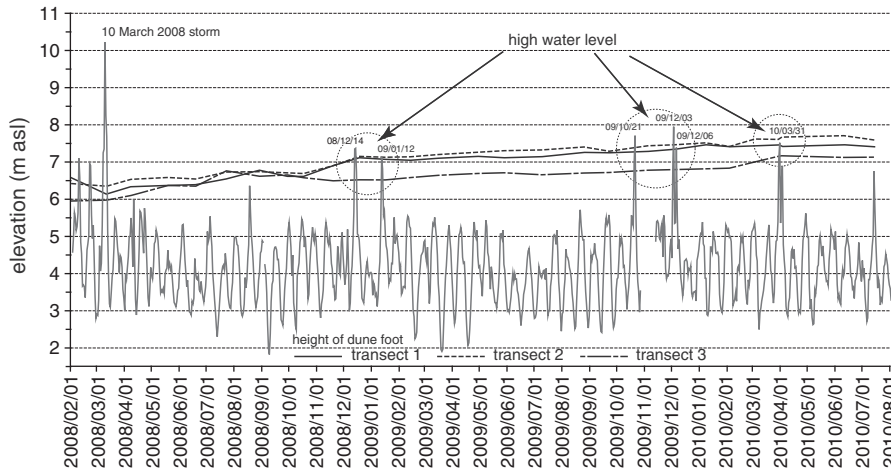


Fig. 14. Comparison between extreme water levels and height of dune toe on Vougot Beach between March 2008 and August 2010.

Duck, North Carolina. Erosion of the upper tidal beach sand sheet has, therefore, led to the exposure of organic-rich freshwater peat layers over a surface increasing between 2008 and 2010. In the long term, these processes could limit sediment transfer between the beach and the dune because, as shown by Ruz and Meur-Ferec (2004), sand moisture content generally increases, due to ground water seepage in the vicinity of the peat layer outcropping at the seaward limit of the upper beach, inducing a limiting factor for aeolian sand transport.

The model proposed in Fig. 18 illustrates the whole processes described above. The first erosive phase, corresponding to the storm of 10th March 2008, was characterised by exceptionally high extreme water levels (surge + run-up) at the coast (4 m above the dune toe) which attacked the dune and generated seaward return currents

(Fig. 18a). Similar observations were made at Formby Point (England) where the most severe episode of frontal dune erosion on record, with up to 14 m of recession, occurred especially during a tide which reached 6.0 m asl on 26th February 1990 and which was associated with mean onshore wind speed of 15–23 m.s<sup>-1</sup> (Pye, 1991; Pye and Blott, 2008). At Vougot Beach, these processes led to major dune retreat (up to 6 m), of which the primary effect was the creation of accommodation space at the dune toe (Fig. 18b). The sediment volume lost by the dune was transferred to the upper tidal beach by shifting the equilibrium profile upward. These processes worked particularly well at transects 1 and 2 where cross-shore transfer was dominant (Fig. 4); they differed for transect 3 where longshore transfer from east to west led to erosion of the upper tidal beach (Suarez and Cariolet, 2010). As shown in Fig. 18b, it is assumed that seaward

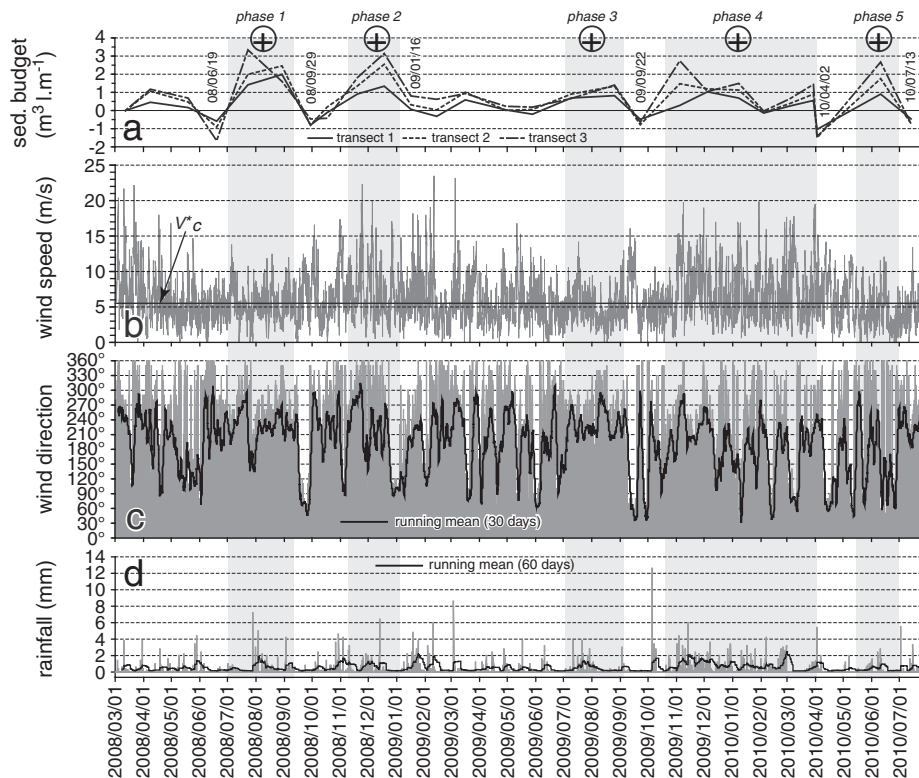


Fig. 15. Meteorological conditions (wind and rainfall) and dune sediment budget measured during the period of survey. Wind and rainfall data obtained from the Météo France meteorological station at Brignogan (see Fig. 1). Dune sediment budget is given for the three transects (see Fig. 4e).

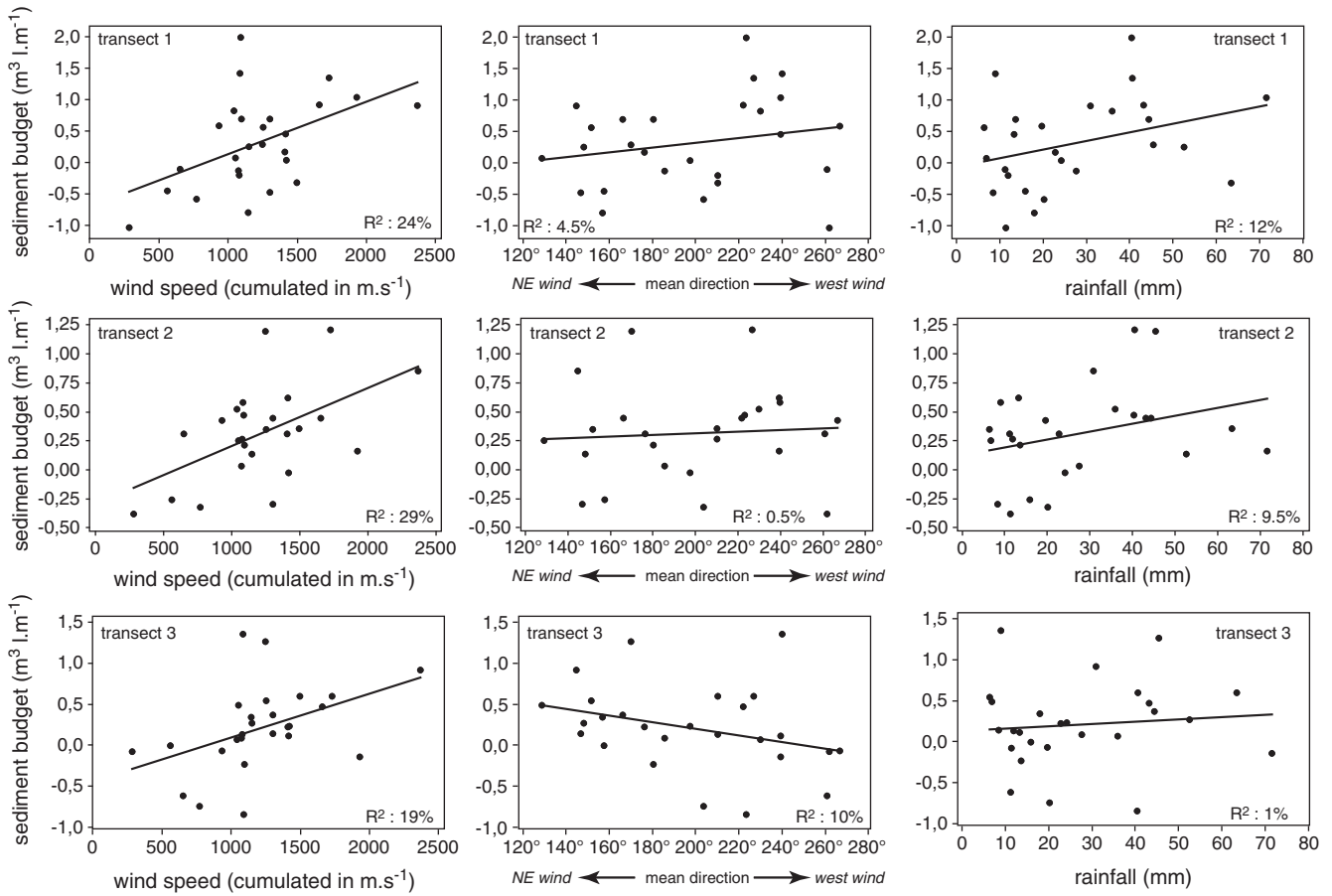


Fig. 16. Correlation between dune sediment budget and wind speed, wind direction and rainfall for the three transects.

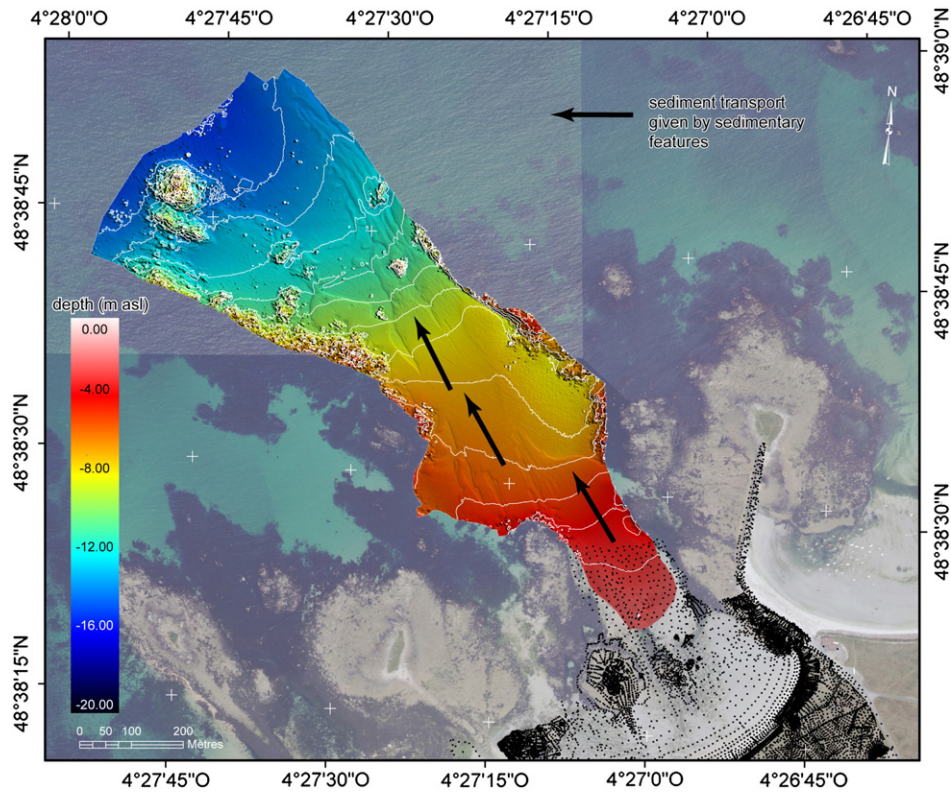


Fig. 17. Bathymetric survey using a multibeam echo sounder conducted on the eastern part of Vougot Beach on 29 July 2010.

return currents generated erosion of the lower tidal beach–nearshore to shoreface zone, which is impossible to quantify as topomorphological monitoring did not cover this area. The second phase illustrates the very rapid dune recovery processes that began in the month following the storm (Fig. 18c). These processes involve aeolian transport resulting in slight dune toe accretion (+0.1 to +0.5 m<sup>3</sup>.m<sup>-1</sup>, see Fig. 10). However, this transport alone cannot explain the strong erosion experienced during this same period by the upper tidal beach at transects 1 and 2 (−10 to −14 m<sup>3</sup>.m<sup>-1</sup>, see Fig. 10). As previously emphasised, the sediment deficit in this eastern section of the beach could be related to transfer between the

lower tidal beach–nearshore to shoreface zone, according to the equilibrium profile readjustment principle; it could also be connected with longshore east–west transport. This transport would explain why, during this period, a positive sediment budget was recorded for the upper tidal beach at transect 3 (Fig. 10). The third phase shows that the above-mentioned processes continued. Two and a half years after the storm of 10th March 2008, the aeolian supply restored an equilibrium within the dune sediment budget, in particular for transects 1 and 2 (Fig. 10), even if the dune continued to retreat at a very low rate (maximum of −0.7 m/year). This sediment supply led to a construction of embryo dunes forming a ‘second line’ of dunes,

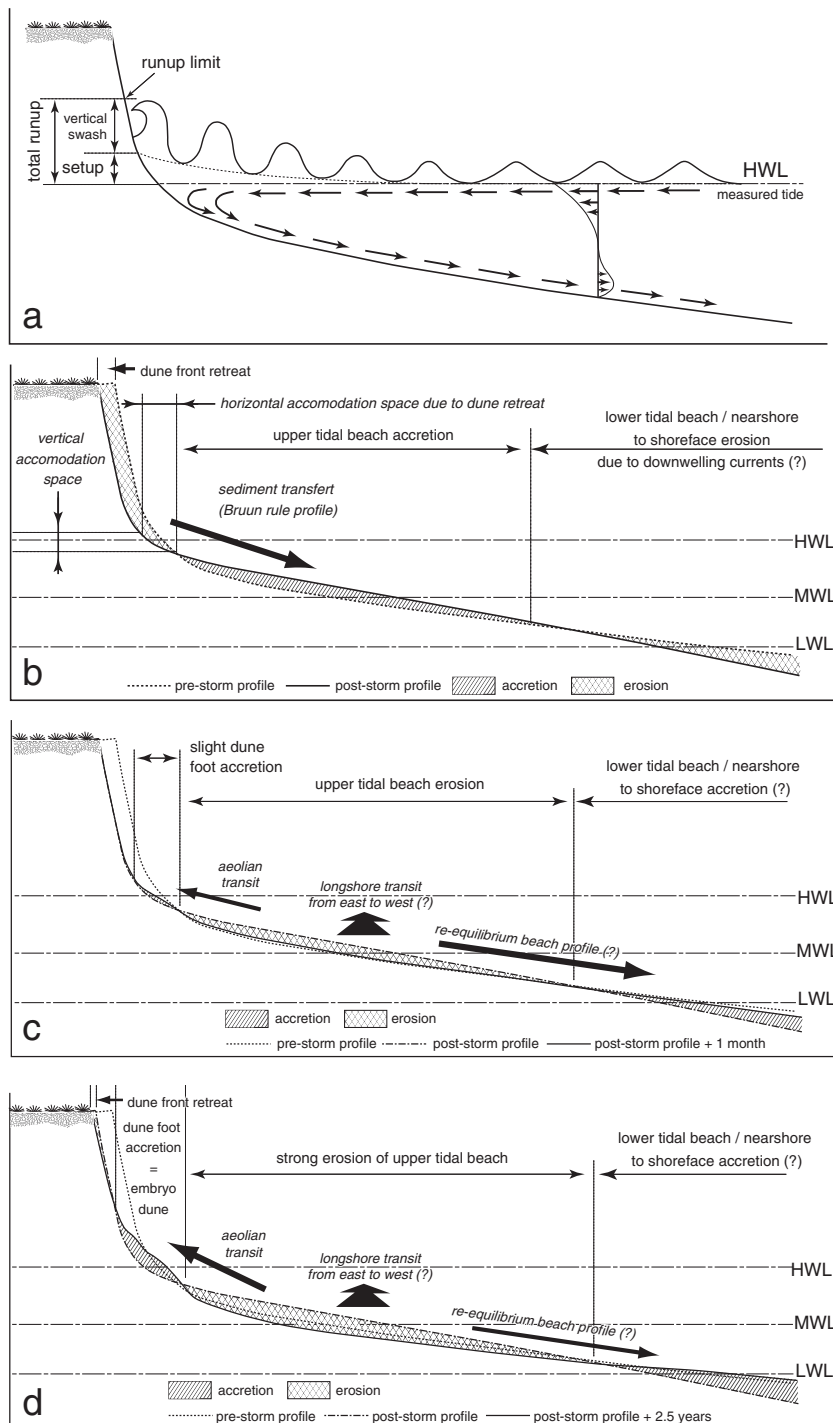


Fig. 18. Morphosedimentary functioning and evolution of the intertidal beach/dune system on Vougot Beach between the storm of 10 March 2008 and the month of July 2010.

facilitated by the creation of accommodation space suitable for sediment storage (Fig. 18d).

Hence, if all these dynamics are entered into the various conceptual models, the dune evolution observed since the storm of 10th March 2008 would match scenario (D) of the Psuty model (Psuty, 1988), characterised by a sediment budget deficit for the entire beach/dune system. In these circumstances, the author indicates that dune erosion is, above all, related to storm surge effect, and that by feedback processes, the increasingly severe lowering of the beach profile promotes more frequent attack on the dune. These processes perfectly illustrate the functioning of the beach/dune system on Vougot Beach, even though, as indicated above, the dune recovery that has been occurring for two and a half years is largely dictated by accommodation space. The creation of this accommodation space, generated by the retreat and, more importantly, elevation of the dune toe, has reduced the effects of wave attack on the dune as uprush processes during storms are, under these circumstances, less frequent and less energetic. However, as indicated by the Hesp model (Hesp, 1988, 2002), these dune recovery phenomena after particularly erosive storms cannot occur for very long periods of time. They generally depend on sediment availability and the frequency of erosive events on a seasonal scale. In the case of Vougot Beach, the sediment stock on the tidal beach that contributed to dune recovery, today appears to be largely depleted.

## 7. Conclusion

The geomorphological analysis performed immediately after the storm of 10th March 2008 reveals a number of key points relating to dune recovery processes:

1. The particularly severe dune erosion during the storm was generated by extreme water levels approximately 4 m higher than the dune toe. These processes caused dune retreat by up to 6 m in places. They also very probably generated seaward return currents which may have eroded the lower tidal beach–nearshore to shoreface zone and transported this sediment seaward.
2. The initiation of the recovery of dunes was immediate and still ongoing two and a half years after the storm. Already existing dunes accreted further due to a large aeolian sand supply. This process led to embryo dunes recovery at an average rate of 4–4.5 cm per month, although average monthly volume changes varied from  $-1$  to  $2 \text{ m}^3 \cdot \text{m}^{-1}$ , and total volume changes reached  $+1,816 \pm 141 \text{ m}^3$  across the studied longitudinal section of about 650 m between November 2008–January 2009 and July 2010. These dune construction processes were rapidly facilitated by vegetation growth which fixed the embryo dunes.
3. The sediment supply to the dune was provided by sand mainly from the upper tidal beach whose erosion reached over 1 m in the eastern part of Vougot Beach for the entire survey period. This sediment transfer was mainly generated by aeolian transport, although nearshore drift currents may have played a role in east to west sediment transfer.
4. Dune regeneration was largely determined by the creation of accommodation space. This space is linked to dune retreat and consequently to dune toe elevation, which occurred during the storm. Dune toe submersion and wave attack phenomena during the 2.5-year monitoring period were greatly reduced, enabling embryo dunes to be formed and maintained as a second line of dunes.

## Acknowledgements

The authors wish to thank the European Union–Natura 2000, DIREN Bretagne, and the District of Guissey that funded this work. Tide data came from SONEL database, and were provided by G. Wöpelmann who we thank. We are grateful to the reviewers for their constructive remarks and suggestions for improvement.

## References

- Aagard, T., Davidson-Arnott, R., Greenwood, B., Nielsen, J., 2004. Sediment supply from shoreface to dunes: linking sediment transport measurements and long-term morphological evolution. *Geomorphology* 60, 205–224.
- Anthony, E.J., Vanhée, S., Ruz, M.-H., 2006. Short-term beach–dune sand budgets on the North Sea coast of France: sand supply from shoreface to dunes, and the role of wind and fetch. *Geomorphology* 81, 316–329.
- Ardhuin, F., Marié, L., Rasclé, N., Forget, P., Roland, A., 2009. Observation and estimation of Lagrangian, Stokes and Eulerian currents induced by wind and waves at the sea surface. *Journal of Physical Oceanography* 39, 2820–2838.
- Ardhuin, F., Rogers, E., Babanin, A., Filipot, J.-F., Magne, R., Roland, A., van der Westhuyzen, A., Queffelec, P., Lefevre, J.-M., Aouf, L., Collard, F., 2010. Semi-empirical dissipation source functions for wind-wave models: part I, definition, calibration and validation. *Journal of Physical Oceanography* 40, 1917–1941.
- Bagnold, R.A., 1941. *The Physics of Blown Sand and Desert Dunes*. Chapman and Hall, London.
- Battjes, J.A., 1971. Run-up distributions of waves breaking on slopes. *ASCE Journal of Waterways, Harbours Coastal Engineering Division* 92, 91–114.
- Battjes, J.A., 1974. Surf similarity. *Proc. 14th Conf. Coastal Eng. ASCE*, 1, pp. 466–479.
- Bradshaw, B.E., Healy, T.R., Dell, P.M., Bolstad, W.M., 1991. Inner shelf dynamics on a storm-dominated coast, East Coromandel, New Zealand. *Journal of Coastal Research* 7, 11–30.
- Camacho-Valdéz, V., Murillo-Jiménez, J.M., Nava-Sánchez, E.H., Turrent-Thompson, C., 2008. Dune and beach morphodynamics at Cabo Falso, Baja California Sur, Mexico: response to natural, Hurricane Juliette (2001) and anthropogenic influence. *Journal of Coastal Research* 24, 553–560.
- Cariolet, J.-M., 2011a. Quantification du runup sur une plage macrotidale à partir des conditions morphologiques et dynamiques. *Géomorphologie: Relief, Environnement, Processus* 1, 95–108.
- Cariolet J.-M. 2011b. Inondation des côtes basses et risques associés en Bretagne : vers une redéfinition des processus hydrodynamiques liés aux conditions météo-océaniques et des paramètres morpho-sédimentaires, Ph.D. thesis, Université de Bretagne Occidentale, Brest, France
- Cariolet, J.-M., Costa, S., Caspar, R., Ardhuin, F., Magne, R., Goasguen, G., 2010. Aspects météo-marins de la tempête du 10 mars 2008 en Atlantique et en Manche. *Norix* 215, 11–31.
- Carter, R.W.G., Stone, G.W., 1989. Mechanisms associated with the erosion of sand dune cliffs, Magilligan, Northern Ireland. *Earth Surface Processes and Landforms* 14, 1–10.
- Carter, R.G.W., Hesp, P.A., Nordstrom, K.F., 1990. Erosional landforms in coastal dunes. In: Nordstrom, K., Psuty, N., Carter, B. (Eds.), *Coastal Dunes. Form and Process*. John Wiley & Sons, England, pp. 217–250.
- Claudino-Sales, V., Wang, P., Horwitz, M.H., 2008. Factors controlling the survival of coastal dunes during multiple hurricane impacts in 2004 and 2005: Santa Rosa barrier island, Florida. *Geomorphology* 95, 295–315.
- Crowell, M., Leatherman, S.P., Buckley, M.K., 1991. Historical shoreline change: error analysis and mapping accuracy. *Journal of Coastal Research* 7, 839–852.
- Dean, R.G., 1991. Equilibrium beach profiles: characteristics and applications. *Journal of Coastal Research* 7, 53–84.
- Edelman, T., 1968. Dune erosion during storm conditions. *Proc. 11th Conf. Coastal Eng. ASCE*, 1, pp. 719–722.
- Edelman, T., 1972. Dune erosion during storm conditions. *Proc. 13th Conf. Coastal Eng. ASCE*, 2, pp. 1305–1311.
- Erikson, L.H., Larson, M., Hanson, H., 2007. Laboratory investigation of beach scarp and dune recession due to notching and subsequent failure. *Marine Geology* 245, 1–19.
- Fisher, J.S., Overton, M.F., 1984. Numerical model for dune erosion due to wave uprush. *Proc. 19th Conf. Coastal Eng., ASCE*, pp. 1553–1558.
- Gayes, P., 1991. Post-Hurricane Hugo nearshore side scan sonar survey, Myrtle Beach to Folly Beach, South Carolina. *Journal of Coastal Research* 8 (SI), 95–111.
- Guilcher, A., Hallégouët, B., 1991. Coastal dunes in Brittany and their management. *Journal of Coastal Research* 7, 517–533.
- Héquette, A., Hill, P.R., 1993. Storm-generated currents and offshore sediment transport on a sandy shoreface, Tibjak Beach, Canadian Beaufort Sea. *Marine Geology* 113, 283–304.
- Héquette, A., Hill, P.R., 1995. Response of the seabed to storm generated combined flows on a sandy arctic shoreface, Canadian Beaufort Sea. *Journal of Sedimentary Research* A65, 461–471.
- Hesp, P.A., 1988. Surfzone, beach and foredune interactions on the Australian southeast coast. *Journal of Coastal Research* 3 (SI), 325–332.
- Hesp, P.A., 2002. Foredunes and blowouts: initiation, geomorphology and dynamics. *Geomorphology* 48, 245–268.
- Holman, R.A., 1986. Extreme value statistics for wave run-up on a natural beach. *Coastal Engineering* 9, 527–544.
- Holman, R.A., Sallenger, A.H., 1985. Set-up and swash on a natural beach. *Journal of Geophysical Research* 90 (C1), 945–953.
- Hotta, S., Kubota, S., Katori, S., Horikawa, K., 1984. Sand transport by wind on a wet sand surface. *Proc. 19th Conf. Coastal Eng. ASCE*, pp. 1263–1281.
- Houser, C., Hamilton, S., 2009. Sensitivity of post-hurricane beach and dune recovery to event frequency. *Earth Surface Processes and Landforms* 34, 613–628.
- Houser, C., Hapke, C., Hamilton, S., 2008. Controls on coastal dune morphology, shoreline erosion and barrier island response to extreme storms. *Geomorphology* 100, 223–240.
- Hunt, I.A., 1959. Design of seawalls and breakwaters. *Journal of Waterways and Harbours Division, ASCE* 85 (WW3), 123–152.
- Kriebel, D.L., 1986. Verification study of a dune erosion model. *Shore & Beach* 54, 13–21.

- Kriebel, D.L., Dean, R.G., 1985. Numerical simulation of time-dependant beach and dune erosion. *Coastal Engineering* 9, 221–245.
- Larson, M., Erikson, L., Hanson, H., 2004. An analytical model to predict dune erosion due to wave impact. *Coastal Engineering* 51, 675–696.
- Lee, G., Nicholls, R.J., Birkemeier, W.A., 1998. Storm-driven variability of beach-nearshore profile at Duck, North Carolina, USA, 1981–1991. *Marine Geology* 148, 163–177.
- Lentz, S.J., Fewings, M., Howd, P., Fredericks, J., Hathaway, K., 2008. Observations and a model of undertow over the inner continental shelf. *Journal of Physical Oceanography* 38, 2341–2357.
- Levin, N., 2011. Climate-driven changes in tropical cyclone intensity shape dune activity on Earth's largest sand island. *Geomorphology* 125, 239–252.
- Levin, N., Ben-Dor, E., 2004. Monitoring sand dune stabilization along the coastal dunes of Ashdod-Nizanim, Israel, 1945–1999. *Journal of Arid Environments* 58, 335–355.
- Namikas, S.L., Sherman, D.J., 1995. A review of the effects of surface moisture content on Aeolian sand transport. In: Tchakerian, V.P. (Ed.), *Desert Aeolian Processes*. Chapman & Hall, New York, pp. 269–293.
- Nielsen, P., Hanslow, D.J., 1991. Wave runup distributions on natural beaches. *Journal of Coastal Research* 7, 1139–1152.
- Overton, M.F., Fisher, J.S., 1988. Laboratory investigation of dune erosion. *Journal of Waterway, Port, Coastal, and Ocean Engineering* 114, 367–373.
- Prietas, A.M., Fagherazzi, S., 2010. Morphological barrier island changes and recovery of dunes after Hurricane Dennis, St. George Island, Florida. *Geomorphology* 114, 614–626.
- Psuty, N.P., 1988. Sediment budget and dune/beach interaction. *Journal of Coastal Research* 3 (SI), 1–4.
- Pye, K., 1991. Beach deflation and backshore dune formation following erosion under storm surge conditions: an example from Northwest England. *Acta Mechanica* 2 (supplement), 171–181.
- Pye, K., Blott, S.J., 2008. Decadal-scale variation in dune erosion and accretion rates: an investigation of the significance of changing storm tide frequency and magnitude on the Sefton coast. *Geomorphology* 102, 652–666.
- Pye, K., Neal, A., 1994. Coastal dune erosion at Formby Point, north Merseyside, England: causes and mechanisms. *Marine Geology* 119, 39–56.
- Ruggiero, P., Komar, P.D., McDouglas, W.G., Marra, J.J., Beach, R.A., 2001. Wave runup, extreme water levels and erosion of properties backing beaches. *Journal of Coastal Research* 17, 407–419.
- Ruz, M.-H., Meur-Ferec, C., 2004. Influence of high water levels on aeolian sand transport: upper beach/dune evolution on a macrotidal coast, Wissant Bay, northern France. *Geomorphology* 60, 73–87.
- Sallenger, A.H., 2000. Storm impact scale for barrier islands. *Journal of Coastal Research* 16, 890–895.
- Sallenger, A., Wright, C.W., Guy, K., Morgan, K., 2004. Assessing storm-induced damage and dune erosion using airborne lidar: examples from Hurricane Isabel. *Shore & Beach* 72, 3–7.
- Saye, S.E., van der Wal, D., Pye, K., Blott, S.J., 2005. Beach–dune morphological relationships and erosion/accretion: an investigation at five sites in England and Wales using LIDAR data. *Geomorphology* 72, 128–155.
- Sherman, D.J., Bauer, B.O., 1993. Dynamics of beach–dune systems. *Progress in Physical Geography* 17, 413–447.
- Sherman, D.J., Jackson, D.W.T., Namikas, S.L., Wang, J., 1998. Wind-blown sand on beaches: an evaluation of models. *Geomorphology* 22, 113–133.
- SHOM-CETMEF. 2008. Statistiques des niveaux marins extrêmes de pleine mer Manche et Atlantique, CD-ROM, Coédition SHOM (Brest) and CETMEF (Plouzané).
- Snedden, J.W., Nummedal, D., Amos, A.F., 1988. Storm- and fairweather combined flow on the central Texas continental shelf. *Journal of Sedimentary Research* 58, 580–595.
- Stockdon, H.F., Holman, R.A., Howd, P.A., Sallenger, A.H., 2006. Empirical parametrization of setup, swash and runup. *Coastal Engineering* 53, 573–588.
- Stockdon, H.F., Sallenger, A.H., Holman, R.A., Howd, P.A., 2007. A simple model for the spatially-variable coastal response to hurricanes. *Marine Geology* 238, 1–20.
- Suarez, S., Cariolet, J.-M., 2010. L'action des tempêtes sur l'érosion des dunes: les enseignements de la tempête du 10 mars 2008. *Noréis* 215, 77–99.
- Suarez, S., Cariolet, J.-M., Fichaut, B., 2010. Monitoring of recent morphological changes of the dune of Vougot Beach (Brittany, France) using differential GPS. *Shore & Beach* 78, 37–47.
- van de Graaff, J., 1977. Dune erosion during a storm. *Coastal Engineering* 1, 99–134.
- van de Graaff, J., 1986. Probabilistic design of dunes; an example from The Netherlands. *Coastal Engineering* 9, 470–500.
- van der Meulen, T., Gourlay, M.R., 1968. Beach and dune erosion test. *Proc. 11th Conf. Coastal Eng. ASCE*, 1, pp. 701–707.
- Vanhée, S., Anthony, E., Ruz, M.-H., 2002. Aeolian sand transport on a ridge and runnel beach: preliminary results from Leffrinckoucke Beach, northern France. *Journal of Coastal Research* 32 (SI), 732–740.
- Vellinga, P., 1982. Beach and dune erosion during storm surges. *Coastal Engineering* 6, 361–387.
- Winant, C.D., 1980. Downwelling over the Southern California shelf. *Journal of Physical Oceanography* 10, 791–799.
- Wright, L.D., Boon, J.D., Kim, S.C., List, J.H., 1991. Modes of cross-shore sediment transport on the shoreface of the Middle Atlantic Bight. *Marine Geology* 96, 19–51.
- Zuzeck, P.J., Nairn, R.B., Thieme, S.J., 2003. Spatial and temporal considerations for calculating shoreline change rates in the Great Lakes Basin. *Journal of Coastal Research* 38 (SI), 125–146.